Shape coexistence and first-forbidden decay of ^{92}Rb to ^{92}Sr

A. Petrovici *

Horia Hulubei National Institute for Physics and Nuclear Engineering, R-077125 Bucharest, Romania

(Received 6 November 2023; accepted 11 January 2024; published 6 February 2024)

The effects of shape coexistence on first-forbidden β^- decay of the 0^- ground state of ^{92}Rb to the 0^+ ground state and 2^+ states in ^{92}Sr were studied within the beyond-mean-field *complex* excited Vampir variational model. The structure of the parent and daughter states and the β-decay properties were investigated using an effective interaction derived from a *G* matrix based on the charge-dependent Bonn CD potential and a large model space. The effects of shape coexistence and mixing revealed by the structure of the involved states on the properties of the investigated ground state to ground state and first-forbidden unique transitions are discussed and comparison to the available data is presented.

DOI: 10.1103/PhysRevC.109.024303

I. INTRODUCTION

Beta decay properties of particular fission products are of special interest due to the open questions concerning the reactor antineutrino anomalies, the ≈6% deficit of the detected antineutrino, and a spectral disagreement of ≈10% excess in the 4–6 MeV range with respect to the theoretical predictions [1–3]. Recently, much interest was devoted to the role of the first-forbidden transitions [4–6]. One of the dominant contributors to the reactor antineutrino spectrum in the 5–8 MeV range is the ^{92}Rb nucleus [7–10], but the structure of its forbidden transitions is still under investigation.

Neutron-rich nuclei in the $A = 100$ mass region display particular variations in their structure and dynamics correlated with the onset of deformation around the $N = 58$ neutron number [11–18]. Sudden changes have been identified in the Sr and Zr isotopic chains, but a smooth transition was identified in the Kr chain. Previous beyond-mean-field studies based on the *complex* excited Vampir variational model evidenced triple shape coexistence in the $N = 58$ ^{96}Sr and ^{98}Zr isotopes [12] and oblate-prolate coexistence and mixing in ^{94}Kr [16]. Recently, the onset of deformation at $N = 57$ was supported by a new isomer in ^{96}Y [17] and triple shape coexistence was found behind the first-forbidden $0^- \rightarrow 0^+$ β^- decay of ^{96}Y to ^{96}Zr [18].

This workstudies exotic phenomena requiring shape coexistence and mixing in neutron-rich nuclei with $N = 54, 55$, aiming toward a comprehensive description of the characteristics of the parent and daughter states and the properties of first-forbidden β^- decay of ^{92}Rb to ^{92}Sr. The properties of the states involved in the first-forbidden decay of the 0^- ground state of ^{92}Rb to the ground state and 2^+ states in ^{92}Sr are investigated within the *complex* excited Vampir variational model with symmetry projection before variation using a realistic effective interaction and a large model space.

In the next section the main ingredients of the *complex* Excited Vampir model, the effective Hamiltonian, and the theoretical formalism for calculating the nuclear matrix elements involved in the investigated first-forbidden β^- decays will be described. In Sec. III the results concerning the investigated β^- transitions and the triple shape coexistence identified in the structure of the states involved in the decay of the 0^- ground state of ^{92}Rb to the ground state and 2^+ states in ^{92}Sr will be discussed. Finally, some conclusions will be presented in Sec. IV.

II. THEORETICAL FRAMEWORK

The *complex* excited Vampir model (EXVAM), a variational approach to the nuclear many-body problem, uses as basic building blocks general symmetry-projected Hartree-Fock-Bogoliubov (HFB) determinants based on essentially complex HFB transformations allowing for neutron-proton, angular momentum, and parity mixing. The use of essentially *complex* transformations provides the possibility to account for arbitrary two-nucleon correlations in the wave functions including proton-neutron pairing correlations in the $T = 0$ and $T = 1$ channels and unnatural-parity correlations. Time-reversal and axial symmetry are imposed on the HFB transformations. The restoration of broken symmetries of the HFB vacua (nucleon numbers, parity, total angular momentum) is done by projection before variation. The resulting symmetry-projected configurations are used as trial wave functions in independent chains of variational calculations built for each considered symmetry in order to determine the underlying HFB transformations ([12] and references therein). The residual interaction between the successively created solutions for a considered symmetry is diagonalized and finally the mixing of the EXVAM configurations is determined. The *complex* excited Vampir beyond-mean-field procedure allows one to find in a small excitation energy interval orthogonal projected configurations displaying different characteristics in the intrinsic system. One can find

*spetro@nipne.ro

 ©2024 American Physical Society

multiple shape coexistence, identifying spherical and differently deformed oblate and prolate configurations successively appearing in the chain of variational calculations corresponding to a particular symmetry. The final diagonalization could produce in the structure of the wave functions strong mixing of the projected configurations manifesting significant correlations. The *complex* excited Vampir model allows one to use large model spaces and realistic effective interactions making possible *large-scale* nuclear structure investigations going far beyond the abilities of the conventional shell-model configuration-mixing approach.

For nuclei in the $A = 100$ mass region one uses a large model space above the ^{40}Ca core built out of the $1p_{1/2}$, $1p_{3/2}$, $0f_{5/2}$, $0f_{7/2}$, $2s_{1/2}$, $1d_{3/2}$, $1d_{5/2}$, $0g_{7/2}$, $0g_{9/2}$, and $0h_{11/2}$ oscillator orbits for both protons and neutrons in the valence space. This model space was successfully used for the investigation of coexistence phenomena manifested by the structure and β decay of neutron-rich $A \approx 100$ nuclei [11–13,16–18].

The effective two-body interaction is constructed from a nuclear matter G matrix based on the Bonn CD potential. To enhance the pairing correlations the G matrix was modified by adding short-range (0.707 fm) Gaussians in the $T = 1$ and $T = 0$ channels. In addition the isoscalar interaction was modified by monopole shifts for the $T = 0$ matrix elements of the form $\langle 0g_{9/2}0f; IT = 0|\hat{G}|0g_{9/2}0f; IT = 0\rangle$ ($0f$ denotes either the $0f_{5/2}$ or the $0f_{7/2}$ orbital), $\langle 0f_{5/2}1d; IT = 0|\hat{G}|0f_{5/2}1d; IT = 0\rangle$ ($1d$ denotes either the $1d_{3/2}$ or the $1d_{5/2}$ orbital), and $\langle 0g_{9/2}0h_{11/2}; IT = 0|\hat{G}|0g_{9/2}0h_{11/2}; IT = 0\rangle$. The Hamiltonian includes the two-body matrix elements of the Coulomb interaction between the valence protons.

The present work investigates the first-forbidden $0^- \to 0^+$ β^- decay of the 0^- ground state of ^{92}Rb to the 0^+ ground state of ^{92}Sr and the first-forbidden unique $0^- \to 2^+$ decay to the 2^+ states in ^{92}Sr.

The partial half-life of a transition is obtained by

$$\frac{1}{t_{1/2}} = \frac{f}{K} \tag{1}$$

with $K = 6146$ s, and the phase factor has the form

$$f = \int_1^{W_0} C(W)W(W^2-1)^{1/2}(W_0 - W)^2 F(Z,W)dW, \tag{2}$$

where $F(Z,W)$ is the Fermi function correcting the phase space integral for the Coulomb distortion of the electron wave function near the nucleus, W is the total—rest mass and kinetic—energy of the electron in units of $m_e c^2$, $\sqrt{W^2-1}$ is the momentum in units of $m_e c$, and W_0 is the maximum electron energy in units of $m_e c^2$.

For the first-forbidden transitions, the shape factor has the form

$$C(W) = k + kaW + kb/W + kcW^2, \tag{3}$$

where the coefficients k, ka, kb, and kc depend on the first-forbidden nuclear matrix elements, the maximum electron energy, and the quantity $\xi = \alpha Z/2R$, where α is the fine-structure constant and R is the nuclear charge radius.

For the first-forbidden transitions of $0^- \to 0^+$ type the shape factor is

$$C(W) = k + kb/W, \tag{4}$$

where the coefficients k and kb depend on the first-forbidden nuclear matrix elements between the initial ($|\xi_i J_i>$) and the final ($|\xi_f J_f>$) states of spin J_i and J_f,

$$O(0^-) = \sum_{ab} o^{(0)}(0^-)(ab)\langle \xi_f J_f||[c_a^\dagger \tilde{c}_b]_0||\xi_i J_i\rangle, \tag{5}$$

composed of the reduced single-particle matrix elements of rank 0 operators, $o^{(0)}(0^-)(ab)$, and the reduced one-body transition densities calculated using the harmonic oscillator wave functions. For β^- decay $c_a^\dagger$ is the proton creation operator and $\tilde{c}_b$ is the neutron annihilation operator and the sum runs over the valence nucleons.

Following Behrens and Bühring [19] and the detailed expressions given in [20,21], the reduced single particle matrix elements occur in the following combinations:

$$k = \zeta_0^2 + \frac{1}{9}w^2, \tag{6}$$

$$kb = \frac{2}{3}\mu_1\gamma_1[-\zeta_0 w], \tag{7}$$

with

$$\begin{aligned} \zeta_0 &= V + \frac{1}{3}wW_0, \\ V &= v + \xi w'. \end{aligned} \tag{8}$$

The parameter $\mu_1 \approx 1$ [22] and γ_1 is given by $\sqrt{1-(\alpha Z)^2}$. The reduced single-particle matrix elements are

$$w = -g_A\sqrt{3}\langle a||r[\boldsymbol{C}_1 \times \boldsymbol{\sigma}]^{(0)}||b\rangle, \tag{9}$$

$$w' = -g_A\sqrt{3}\langle a||\tfrac{2}{3}rI(1,1,1,1,r)[\boldsymbol{C}_1 \times \boldsymbol{\sigma}]^{(0)}||b\rangle, \tag{10}$$

$$v = \frac{\epsilon_{\rm mec} g_A\sqrt{3}}{M}\langle a||[\boldsymbol{\sigma} \times \boldsymbol{\nabla}]^{(0)}||b\rangle, \tag{11}$$

where $g_A = 1.26$, $\boldsymbol{\sigma}$ is the Pauli spin operator,

$$\boldsymbol{C}_{lm} = \sqrt{\frac{4\pi}{2l+1}}\boldsymbol{Y}_{lm}, \tag{12}$$

with $\boldsymbol{Y}_{lm}$ the spherical harmonics, M is the nucleon mass, and the Coulomb factor taking into account the nuclear charge distribution approximated by a uniform spherical distribution is given by [22]

$$I(1,1,1,1,r) = \frac{3}{2}\begin{cases} 1 - \frac{1}{5}(\frac{r}{R})^2, & 0 \leqslant r \leqslant R, \\ \frac{R}{r} - \frac{1}{5}(\frac{R}{r})^3, & r \geqslant R. \end{cases} \tag{13}$$

The enhancement of the timelike component of the axial current matrix elements by the meson-exchange currents [23,24] is denoted by $\epsilon_{\rm mec}$.

TABLE I. The amount of mixing of the lowest *complex* excited Vampir 2^+ states of ^{92}Sr. The contributions (of at least 2%) of prolate and oblate deformed EXVAM configurations are indicated in decreasing order.

I ($\hbar$)	Prolate content	Oblate content
2_1^+	65(6)%	19(5)%
2_2^+	24(2)(2)%	71%
2_3^+	59(28)(5)%	4%
2_4^+	22(17)(16)(2)%	32(4)%
2_5^+	39(6)(4)(2)(2)%	33(4)(2)%
2_6^+	46(7)(3)(2)%	22(7)(4)(2)%
2_7^+	8(4)(3)(2)(2)%	67(8)%
2_8^+	25(7)(6)(5)(5)(2)(2)%	17(14)(10)(2)%
2_9^+	22(22)(7)(7)(3)%	18(9)(4)(2)%
2_{10}^+	24(12)(3)(2)(2)%	22(10)(3)(2)(2)%
2_{11}^+	28(26)(17)(3)(3)%	5(3)(3)(2)(2)%
2_{12}^+	9(8)(7)(4)(3)(2)(2)(2)%	33(12)(11)(4)(2)%

For the first-forbidden transitions of $0^- \to 2^+$ type the shape factor is

$$C(W) = k + kaW + kcW^2, \tag{14}$$

where the coefficients k, ka, and kc depend on the first-forbidden nuclear matrix elements of rank 2 operator

$$O(0^-) = \sum_{ab} o^{(2)}(0^-)(ab)\langle \xi_f J_f || [c_a^\dagger \tilde{c}_b]_2 || \xi_i J_i \rangle. \tag{15}$$

The reduced single particle matrix elements occur in the following combinations:

$$k = \frac{1}{12} z^2 \left(W_0^2 - \lambda_2\right), \tag{16}$$

$$ka = -\frac{1}{6} z^2 W_0, \tag{17}$$

$$kc = \frac{1}{12} z^2 (1 + \lambda_2), \tag{18}$$

with

$$z = 2 g_A \langle a || r[\boldsymbol{C}_1 \times \boldsymbol{\sigma}]^{(2)} || b \rangle, \tag{19}$$

The approximation $\lambda_2 \approx 1$ [22] is used.

III. RESULTS AND DISCUSSION

The EXVAM results unveil a large variety of configurations building the many-nucleon basis for each considered symmetry. The final solutions were obtained by diagonalizing the residual interaction between the *complex* excited Vampir configurations successively constructed for each spin-parity in independent chains of variational calculations.

TABLE II. The $\log ft$ values for the decay of the 0^- ground state of ^{92}Rb to the 0^+ ground state of ^{92}Sr for different $\epsilon_{\rm mec}$ values compared to data [25].

$\epsilon_{\rm mec} = 1.3$	$\epsilon_{\rm mec} = 1.4$	$\epsilon_{\rm mec} = 1.5$	Expt.
5.92	5.78	5.66	5.75

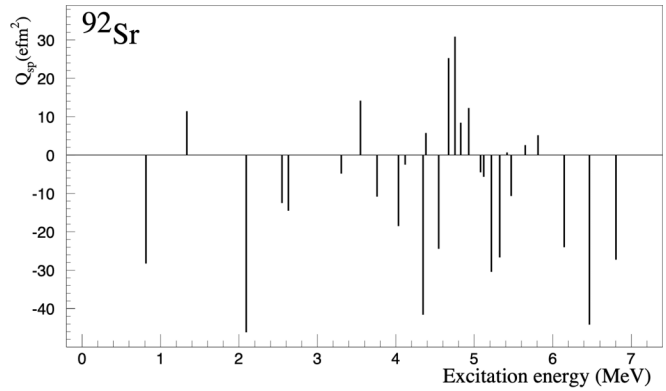

FIG. 1. Spectroscopic quadrupole moments of the 2^+ daughter states in ^{92}Sr.

In ^{92}Rb the wave function of the 0^- ground state is built out of a single spherical configuration characterized on the neutron side by 4.81 particle occupation of the $1d_{5/2}$ spherical orbital. Prolate and oblate deformed configurations in the intrinsic system dominate the structure of the excited 0^- states in ^{92}Rb.

In ^{92}Sr, for the description of the 0^+ ground state a many-nucleon basis of dimension 13 was constructed, while the EXVAM basis for the 2^+ states was built out of 28 projected configurations. In ^{92}Sr the EXVAM results reveal triple shape coexistence in the structure of the 0^+ ground state: The spherical component represents 57%, the deformed prolate configurations make 28%, and the oblate ones 15% of the total amplitude. The structure of the wave functions for the investigated 2^+ states in ^{92}Sr indicates variable, for some states strong, oblate-prolate mixing. Table I illustrates the contribution of different prolate and oblate deformed configurations in the intrinsic system as percentages of the total amplitude for the lowest 12 states of spin 2^+. The amount of mixing of the configurations contributing at least 2% to the structure of the wave function for each state is indicated in decreasing order. The results display a complex structure involving many more differently deformed configurations with increasing excitation energy. In the intrinsic system the quadrupole deformation parameter of the configurations building the structure of the 2^+ states varies from $\beta_2 = 0.06$ to $\beta_2 = 0.31$ for the prolate deformed ones, while for the oblate deformed ones it varies from $\beta_2 = -0.18$ to $\beta_2 = -0.25$.

The spectroscopic quadrupole moments for the calculated 2^+ daughter states using the effective charges $e_p = 1.1$ and $e_n = 0.1$ are depicted in Fig. 1. For the excitation energy of the yrast 2^+ state the experimental value was assumed (250 keV lower than the EXVAM value), and for the other states the relative value with respect to the yrast state was assumed. The density of the 2^+ states is increasing with excitation energy, reaching a maximum in the 4.0–5.5 MeV interval as illustrated in Fig. 1. The small spectroscopic quadrupole values displayed in Fig. 1 for particular 2^+ states could be correlated with the strong oblate-prolate mixing in the structure of the corresponding wave functions presented in Table I.

TABLE III. The log ft values for the decay of the 0^- ground state of ^{92}Rb to the 0^+ ground state of ^{92}Sr for different $\epsilon_{\rm mec}$ values constraining the structure of the final state, 0^+, to 100% spherical, 100% prolate, and 100% oblate content.

	$\epsilon_{\rm mec} = 1.3$	$\epsilon_{\rm mec} = 1.4$	$\epsilon_{\rm mec} = 1.5$
$0^+_{\rm spherical}$	5.62	5.49	5.37
$0^+_{\rm prolate}$	7.57	7.45	7.34
$0^+_{\rm oblate}$	9.15	9.06	9.02

The calculated $B(E2; 2^+_1 \rightarrow 0^+_{\rm gs})$ value is 277 e^2fm^4, while the experimental value amounts to 197(74) e^2fm^4 [25].

The present work investigates the first-forbidden $0^- \rightarrow 0^+$ decay of the ground state of ^{92}Rb to the 0^+ ground state of ^{92}Sr, taking into account the nuclear medium effect on the timelike component of the axial current using the meson-exchange enhancement factor $\epsilon_{\rm mec}$ while keeping the g_A value unquenched. The main contribution is brought by the $d^\nu_{5/2}f^\pi_{5/2}$ matrix element, while very small effects are introduced by the contribution of the $s^\nu_{1/2}p^\pi_{1/2}$, $d^\nu_{3/2}p^\pi_{3/2}$, and $g^\nu_{7/2}f^\pi_{7/2}$ matrix elements. In Table II the results are presented for three values of $\epsilon_{\rm mec}$: 1.3, 1.4, and 1.5. The results for the log ft value indicate that the best agreement with the data, taking into account the ground state feeding of 95.2% and $Q_{\beta^-} = 8.095$ MeV [25], is obtained for $\epsilon_{\rm mec} = 1.4$.

One can make a particular analysis revealing the effects of the shape mixing on the log ft values for the decay of the 0^- ground state of ^{92}Rb to the 0^+ ground state of ^{92}Sr for the three $\epsilon_{\rm mec}$ values, constraining the final state, 0^+, to be built 100% by the spherical configuration, 100% by the main prolate configuration, and 100% by the main oblate configuration found in the EXVAM structure of the wave function for the 0^+ state, constructed using the many-nucleon basis of dimension 13 mentioned above. The results are presented in Table III.

Table IV presents the EXVAM log ft values for the decay of the 0^- ground state of ^{92}Rb to 2^+ states of ^{92}Sr compared to available data [25]. The excitation energy of the yrast 2^+ state is slightly changed to the experimental value (the shift amounts to 250 keV), while for the other states the relative values with respect to the yrast one are considered. The EXVAM results reveal first-forbidden unique branches feeding 2^+ states situated in the high-energy portion of the spectrum, above 5 MeV excitation energy, where significant beta intensity was obtained with total absorption spectroscopy (TAS) measurements [8]. The analysis of the structure of the strongest $0^- \rightarrow 2^+$ transitions indicates dominant contribution coming from the $d^\nu_{5/2}f^\pi_{5/2}$ matrix element. Additional smaller contributions, or canceling effects, are brought by the $d^\nu_{5/2}p^\pi_{1/2}$, $d^\nu_{5/2}p^\pi_{3/2}$, and $g^\nu_{7/2}f^\pi_{5/2}$ matrix elements.

TABLE IV. The log ft values for the decay of the 0^- ground state of ^{92}Rb to 2^+ states of ^{92}Sr compared to available data [25]. The EXVAM excitation energy (in MeV) of the yrast 2^+ state is lowered by 0.250 MeV to the experimental value and for the other states the relative values with respect to the yrast state are considered.

$E^{\rm EXVAM}_{\rm exc}$	$E^{\rm Expt.}_{\rm exc}$	EXVAM	Expt.
0.815	0.815	9.66	9.63
1.337	1.385	10.11	9.77
2.094	1.778	11.60	10.19
2.547	2.054	10.03	10.57
2.631		11.52	
3.303		9.43	
3.550		11.03	
3.761		9.45	
4.032		10.98	
4.120		9.44	
4.348		11.88	
4.385		9.28	
4.545		10.19	
4.674		9.93	
4.755		9.84	
4.826		10.98	
4.927		8.83	
5.079		9.36	
5.119		8.83	
5.219		8.82	
5.322		8.99	
5.417		9.06	
5.470		8.68	
5.650		9.45	
5.814		9.00	
6.147		9.49	
6.469		9.68	
6.805		8.66	

IV. CONCLUSION

This work presents the first comprehensive results obtained within the beyond-mean-field *complex* excited Vampir model concerning the effects of shape coexistence and mixing identified in the structure of the 0^+ ground state and the investigated 2^+ states in ^{92}Sr on their properties as well as on the first forbidden β^- decay of the 0^- ground state of ^{92}Rb to the 0^+ ground state and 2^+ states of ^{92}Sr. The investigation involves a realistic effective interaction and a large model space. Since ^{92}Rb is considered to make a dominant contribution to the reactor antineutrino spectrum in the 5–8 MeV range [7], given the present lack of microscopic knowledge of the first-forbidden transitions, the present results could provide a relevant input for the investigation of the reactor antineutrino spectra. The EXVAM results indicate significant first-forbidden unique transition strengths in the high-energy portion of the spectrum, as also suggested by the data giving support to the present scenario concerning the evolution of shape coexistence and mixing with increasing excitation energy of 2^+ states in ^{92}Sr.

ACKNOWLEDGMENTS

This work was supported by a grant of the Ministry of Research, Innovation and Digitalization, CNCS-UEFISCDI, Project No. PN-III-P4-PCE-2021-0060, within PNCDI III.

[1] Th. H. Mueller *et al.*, Phys. Rev. C **83**, 054615 (2011).
[2] P. Huber, Phys. Rev. C **84**, 024617 (2011).
[3] G. Mention, M. Fechner, Th. Lasserre, Th. A. Mueller, D. Lhuillier, M. Cribier, and A. Letourneau, Phys. Rev. D **83**, 073006 (2011).
[4] A. C. Hayes, J. L. Friar, G. T. Garvey, Gerard Jungman, and G. Jonkmans, Phys. Rev. Lett. **112**, 202501 (2014).
[5] D.-L. Fang and B. A. Brown, Phys. Rev. C **91**, 025503 (2015).
[6] L. Hayen, J. Kostensalo, N. Severijns, and J. Suhonen, Phys. Rev. C **99**, 031301(R) (2019).
[7] A. A. Sonzogni, T. D. Johnson, and E. A. McCutchan, Phys. Rev. C **91**, 011301(R) (2015).
[8] A. A. Zakari-Issoufou *et al.*, Phys. Rev. Lett. **115**, 102503 (2015).
[9] B. C. Rasco *et al.*, Phys. Rev. Lett. **117**, 092501 (2016).
[10] M. Ramalho, J. Suhonen, J. Kostensalo, G. A. Alcala, A. Algora, M. Fallot, A. Porta, and A. A. Zakari-Issoufou, Phys. Rev. C **106**, 024315 (2022).
[11] A. Petrovici, K. W. Schmid, and A. Faessler, Prog. Part. Nucl. Phys. **66**, 287 (2011).
[12] A. Petrovici, Phys. Rev. C **85**, 034337 (2012).
[13] D. Jordan *et al.*, Phys. Rev. C **87**, 044318 (2013).
[14] E. Clément *et al.*, Phys. Rev. Lett. **116**, 022701 (2016).
[15] M. Albers *et al.*, Phys. Rev. Lett. **108**, 062701 (2012).
[16] A. Petrovici, Phys. Scr. **92**, 064003 (2017).
[17] Ł. W. Iskra *et al.*, Europhys. Lett. **117**, 12001 (2017).
[18] A. Petrovici and A. S. Mare, Phys. Rev. C **101**, 024307 (2020).
[19] H. Behrens and W. Bühring, Nucl. Phys. A **162**, 111 (1971).
[20] T. Suzuki, T. Yoshida, T. Kajino, and T. Otsuka, Phys. Rev. C **85**, 015802 (2012).
[21] Q. Zhi, E. Caurier, J. J. Cuenca-García, K. Langanke, G. Martínez-Pinedo, and K. Sieja, Phys. Rev. C **87**, 025803 (2013).
[22] H. Behrens and W. Bühring, *Electron Radial Wave Functions and Nuclear β-Decay* (Clarendon, Oxford, 1982).
[23] H. Mach, E. K. Warburton, R. L. Gill, R. F. Casten, J. A. Becker, B. A. Brown, and J. A. Winger, Phys. Rev. C **41**, 226 (1990).
[24] J. Kostensalo and J. Suhonen, Phys. Lett. B **781**, 480 (2018).
[25] C. M. Baglin, Nucl. Data Sheets **113**, 2187 (2012).